JOURNAL OF MATERIALS SCIENCE 30 (1995) 5514–5521

Synthesis of Fe_3N by mechano-chemical reactions between iron and organic $H_x(CN)_6$ ring compounds

W. A. KACZMAREK, B. W. NINHAM
Research School of Physical Sciences and Engineering, Australian National University, Canberra, ACT 0200, Australia

I. ONYSZKIEWICZ
Institute of Physics, A. Mickiewicz University, 60-780 Poznan, Poland

Novel mechanically activated solid state synthesis reactions between elemental αFe powder and amine compounds–piperazine ($H_{10}C_4N_2$) and pyrazine ($H_4C_4N_2$) – have been studied. Powder samples prepared after 144 and 228 h of ball milling in vacuum were examined by X-ray diffraction, scanning electron microscopy and thermal analysis methods. After ball milling for a time brief compared to that required for most solid state–gas reactions formation of a crystalline iron nitride (Fe_3N) a predominant phase with nitrogen concentration up to ca. 9.0 wt % was observed. Thermal analysis experiments showed structural stability of the Fe_3N phase up to ca. 720 K. In the final product a small residual fraction was formed from αFe and carbon dispersed during mechanical processing. The concentration of carbon in this fraction, estimated from thermogravimetric analysis was up to 2.5 wt %, dependent on milling conditions and the organic compound used. Mechano-chemical synthesis, reaction effectiveness, product composition and particle morphology depends on the milling time and chemical characteristics of the organic compound used. Fine Fe_3N particles at a submicrometre size range were obtained only by milling with pyrazine. Further, the higher chemical reactivity of pyrazine than piperazine was confirmed through the higher level of nitridation achieved in the same preparation time.

1. Introduction

A variety of different thermally activated chemical methods [1] are used for producing thin surface nitride layers. Nitrides are generally less stable than oxides, the affinity of iron for oxygen being greater than that for nitrogen. This higher stability of oxides relative to nitrides dictates that nitrides should be prepared at a lower temperature than oxides and, further, that oxygen and water must be completely excluded from the nitriding environment. With traditional high temperature nitridation techniques it is difficult to produce bulk quantities of nitrides with homogeneous physical properties. Recently, a new method of nitridation involving mechanical alloying was reported [2, 3]. This preparation procedure involves room temperature direct reaction of transition metals in a N_2 or NH_3 atmosphere. In particular, for iron, this method admits the possibility of accessing a wide range of phase compositions, more or less pure, with respect to nitrogen content [4]. The crystal structure of Fe_xN compounds are generally close-packed arrays of the larger Fe atoms, with the smaller nitrogen atoms in the interstitial voids [5]. Iron nitrides have high hardness, thermal and electrical conductivity. This fact, taken together with the possibility (known for two decades) of achieving higher magnetic saturation than for iron or its oxides, suggests that these materials have widespread untapped technical potential. Our interest in these powders is focused on both the technology of nitride preparation and the improvement of their magnetic properties. So far only three phases, $Fe_{16}N_2$, Fe_3N and $\gamma' Fe_4N$, have been investigated for magnetic applications [5–11]. The first compound, which has an abnormally high magnetization, is still extremely difficult to prepare in bulk because of instability of the structure [5–7]. The second has only fair to average ferromagnetic characteristics [8]. The third phase has been found to be a suitable replacement material for reactive iron pigments in high density magnetic recording [9–11]. We have investigated the possibility of bulk iron nitride synthesis, particularly those compounds with 4:1 stoichiometry.

It was proposed recently that transition metal nitrides (especially those belonging to the iron group) can form solid solutions with other isotypical nitrides, carbides, and oxides [12]. In this study carbon- and nitrogen-containing Fe compounds were obtained in powder form. It was therefore possible to investigate the formation and thermal properties of iron nitride and carbide multiphase composite materials formed as a result of solid state reactions. In the preparation

0022–2461

we used highly reactive benzene-type (pyrazine) and cyclohexane-type (piperazine) organic compounds that belong to the amine group. In these, the two carbon atoms at positions 1 and 4 are replaced by nitrogen atoms. These nitrogen-containing molecules are thermally unstable at elevated temperatures above ca. 350 K, and form a variety of simple H_xC-, H_xN- or CN- radicals and side-chains. It was assumed that, with mechanical activation energy transferred to the mixture in the presence of highly reactive transition metal surfaces formed in the milling process, decomposition could be accelerated. Hence, mechanochemical exchange reactions can be expected to be more efficient for nitrides than for the solid–gas reactions used so far. Further, what is expected in this situation is a high value of surface density of active carbon- and nitrogen-containing molecules and radicals as compared to the rather low values (depending on gas pressure) widely used in solid state–gas milling technology. This can be a most important factor in effecting decreased milling time, and in increasing both reaction effectiveness and product morphological characteristics.

2. Experimental procedure

The milling for all samples (ca. 6 g in weight) was conducted in a vertical stainless steel mill (Uni-Ballmill) operating in its high energy mode [13]. The Cr-hardened steel balls (4) have a powder weight ratio of ca. 40:1. But by the application of an external magnetic field, the effective mass of the ferromagnetic balls was increased during preparation by a factor of ca. 80 (from 60 g up to 5 kg). For additional preparation details concerning the ball milling set-up (magnetic field configuration) see ref. 14.

In this study dry milling was performed on pure iron powder [99.99 at %; particle size range 1–10 μm (mean size 4 μm)]; and organic ring-type compounds [piperazine ($H_{10}C_4N_2$) and pyrazine ($H_4C_4N_2$) powders, respectively]. Structural formulas of piperazine and pyrazine are shown in Fig. 1. The amount of piperazine or pyrazine compounds used in the experiments was chosen to satisfy the stoichiometric ratio Fe:N = 4:1, as for $\gamma' Fe_4N$. Chemicals, obtained from Sigma and Aldrich Ltd, were of analytical grade. They were introduced into the vial and sealed after vacuum evacuation at 5×10^2 Pa. After 144 and 288 h of milling a small quantity of material was removed under argon for immediate structure and thermal analysis. Particle morphology was examined by direct observation of gold-coated (20 nm) samples on a Jeol SEM 6400 scanning electron microscope. The structural characterization was performed using a Philips X-ray powder diffractometer employing CoK_α ($\lambda = 1.789$ nm) radiation (scan rate $2° \text{ min}^{-1}$) with a CD-ROM JCPDS-ICDD database and PC fitting program for detailed analysis of XRD patterns. The calorimetric and thermogravimetric experiments were performed in Shimadzu DSC-50 and TGA-50H thermoanalysis system, on ca. 20 mg of material under dynamic pure argon atmosphere at a flow rate 50 ml min^{-1} and a scan rate of $5° \text{ min}^{-1}$.

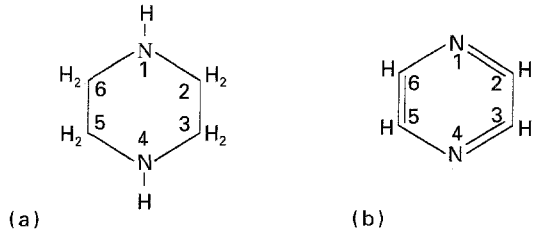

Figure 1 Structural formulas of (a) piperazine and (b) pyrazine.

3. Results and discussion

3.1. Scanning electron microscopy (SEM)

SEM images of the initial αFe and as-prepared powders (milled and annealed) are shown in Figs 2 and 3. The micrographs show irregular particles. The milling time or type of amine compound used in the preparation had an influence on observed size changes. With increasing milling time the average particle size decreased. Particle size was found to be in the range 0.5–10 and 0.3–5 μm (milling time 144 h) for αFe–piperazine and αFe–pyrazine, respectively. Particle sizes for powders milled for 288 h were substantially smaller for αFe–pyrazine powder (0.2–1 μm) than for αFe–piperazine, for which most particles remained in the same 0.3–5 μm range. SEM analysis of powders annealed at 673 and 1273 K show that αFe–piperazine powders retain a similar size distribution and range. By contrast to this invariance of αFe–piperazine ball-milled powders to heat treatment, the αFe–pyrazine samples evidence a remarkable change in particle size. Thus, for powder annealed at 673 K the particle size decreased to an estimated 0.1–1 μm. A major fraction of the smallest particles

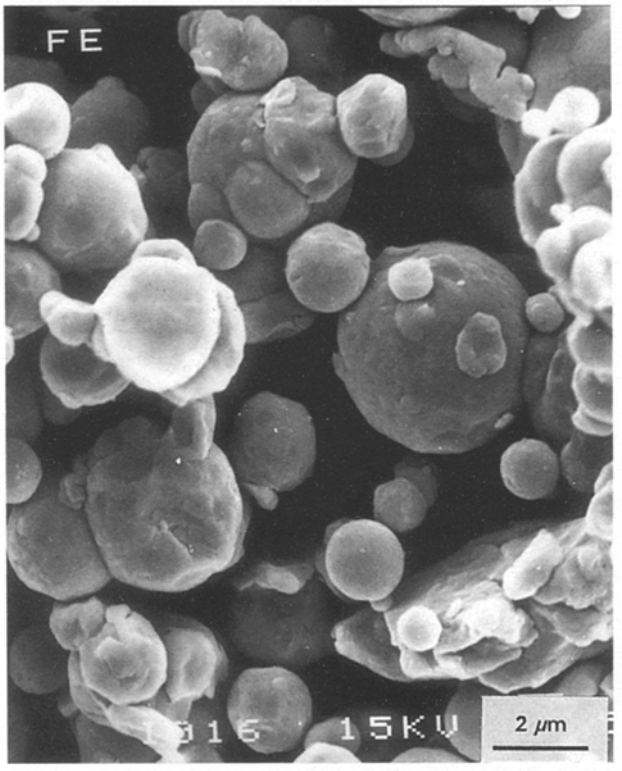

Figure 2 SEM image of αFe powder used in this experiment.

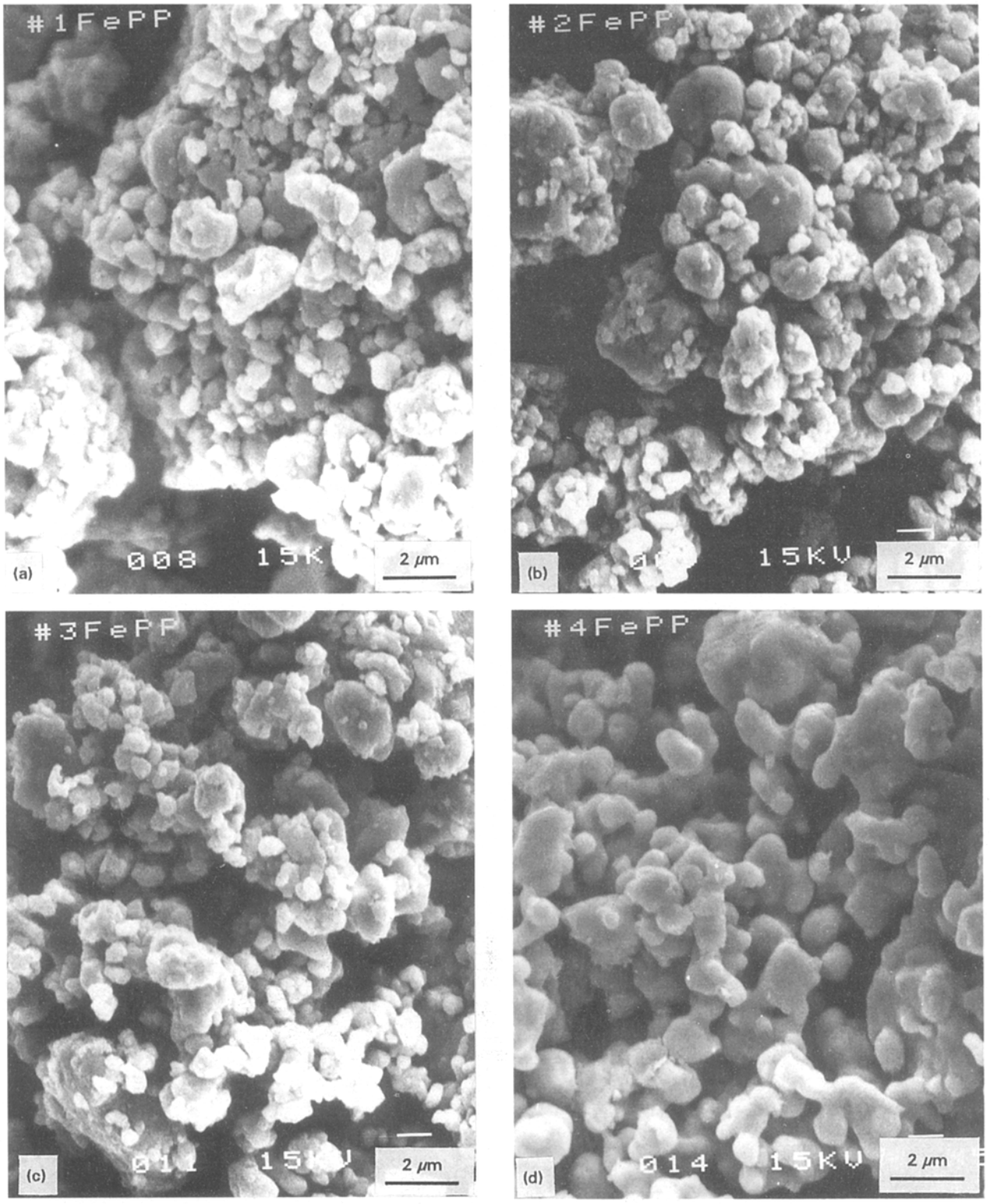

Figure 3 SEM images of αFe–piperazine (a–d) and αFe–pyrazine (a1–d1) powders obtained after: (a) 144 h ball milling in vacuum; (b) 288 h ball milling in vacuum; (c) 15 min annealing at 673 K in an argon atmosphere; (d) TGA scan, sample annealed to 1273 K in an argon atmosphere.

were < 0.5 μm in size. Heat treatment at 1273 K induced a recrystallization process, and the particle size then increased dramatically (1–20 μm). This effect was found to occur only for the αFe–pyrazine powder.

3.2. X-ray diffraction (XRD) analysis of ball-milled αFe–piperazine mixtures

XRD spectra for powders milled with piperazine and subsequently annealed are shown in Fig. 4. It can be seen that the diffraction spectrum for the first 144 h of milling shows minimal changes as compared to pre-milled αFe powder (Fig. 4d can be taken as typical for iron powder). In the range of scattering angles studied, three clearly visible lines are characteristic for αFe. For the 144 h milled samples, only XRD line broadening and relative intensity changes occur, but the peak positions remain at the same scattering angles. It can therefore be assumed that both effects can be attributed to mechanically-activated decrease of crystal

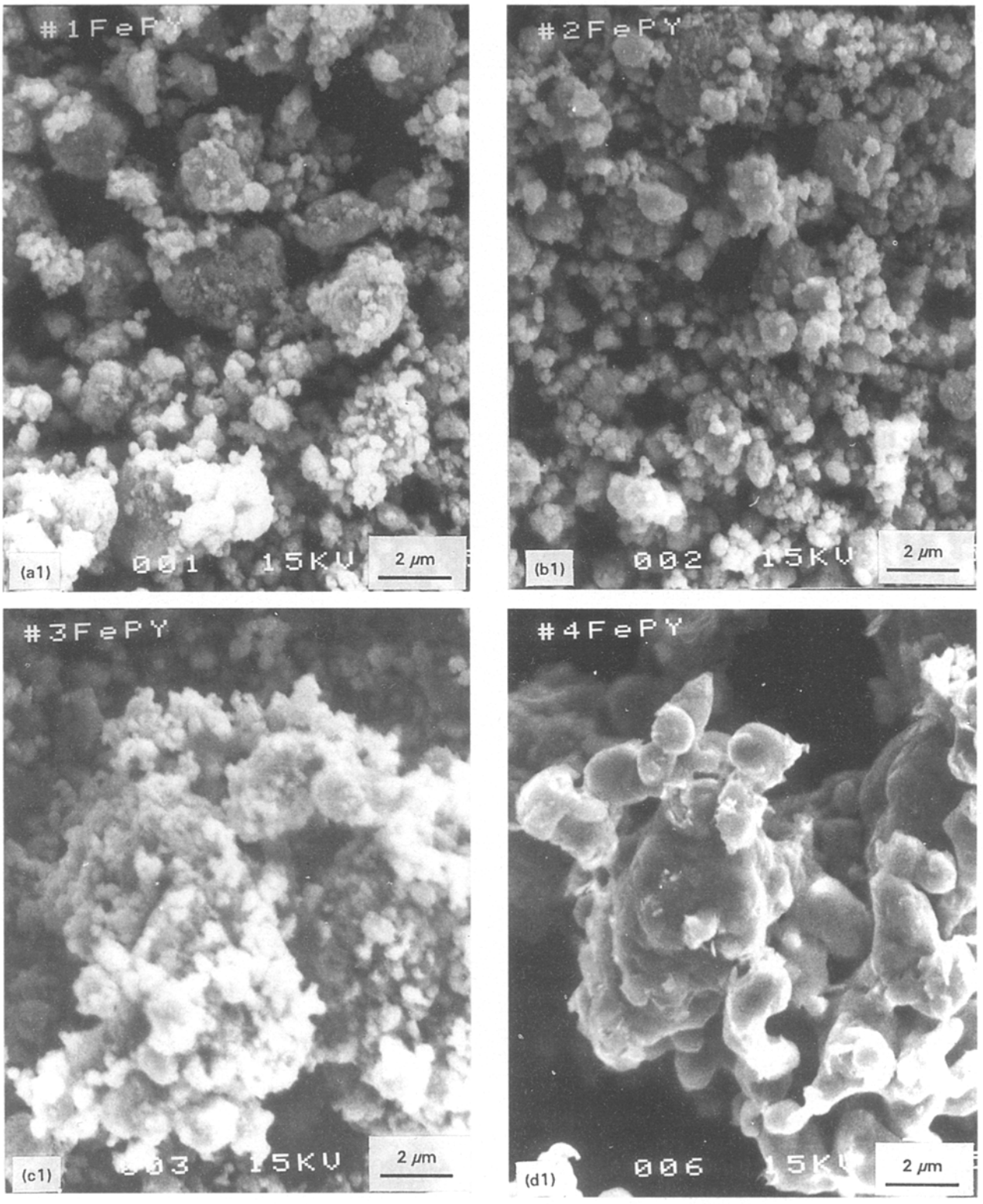

Figure 3 Continued.

grain size and to an increase of crystal structure defect density. This kind of behaviour is characteristic of mechanically alloyed materials with simple cubic structures (bcc for αFe). For our mixture it indicates an absence of chemical reaction between components.

For a sample milled for 288 h a totally different XRD pattern was recorded (cf. Fig. 4b); in this powder two phases were found. The main phase is iron nitride (Fe_3N), and the second shows residual traces of αFe. For iron only the most intense XRD line (1 1 0) can be observed. In Fig. 4 arrows mark all XRD peak positions for the Fe_3N phase, a hexagonal system (hcp) with space group $P6_3/mmc$ [15]. There is good agreement between our results (peak position and relative intensity) and tabulated values. Calculated unit cell values of $a = 0.2739$ nm and $c = 0.4377$ nm are in good agreement with diffraction file data ($a = 0.2695$ nm and $c = 0.4362$ nm). No other phases were found.

A similar mechanism of Fe_3N phase formation was recently described for mechanically alloyed αFe in an

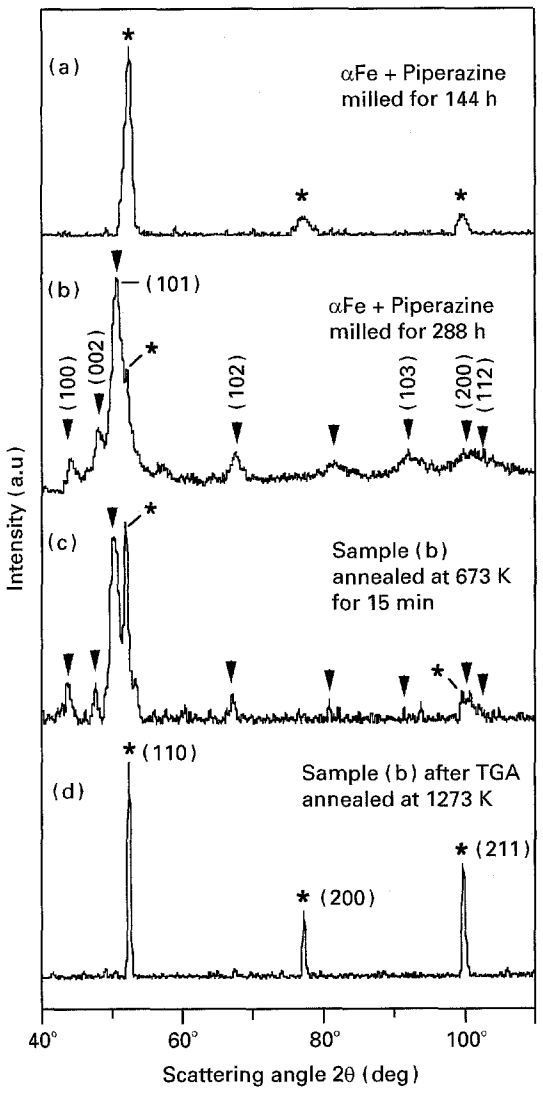

Figure 4 XRD patterns of αFe–piperazine powders (*): α–Fe; (▼): Fe_3N.

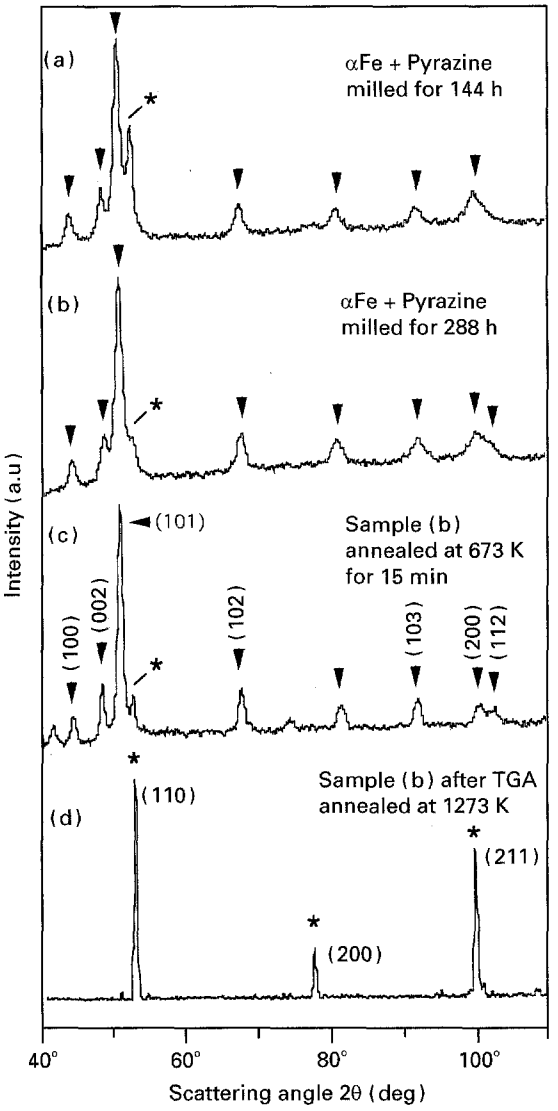

Figure 5 XRD patterns of αFe–pyrazine powders (*): α–Fe; (▼): Fe_3N.

NH_3 atmosphere [8]. However, it is evident that our nitridation process occurs more rapidly if consideration is taken of milling time. In ref. 8 an XRD pattern similar to that shown in Fig. 4a was described as super-saturated iron–nitrogen phase which, under further milling, transformed directly to the Fe_3N phase without any iron contamination. Without going too far into a comparison of αFe mechanically alloyed in NH_3 atmosphere, we emphasize again that for the αFe–piperazine mixture the process has a very different dependence of milling time. It is assumed that in this case, with mechanical activation, significant grain refinement and stress related disordering occurs in the powder particles. The nitridation chemical reaction takes place in parallel with this process. The increasing dislocation and vacancy density in milled αFe induces a situation favourable for direct chemical nitride synthesis following decomposition of the organic molecules (piperazine). In this situation, even for a 288 h milled sample, the main peak line (1 1 0) of the αFe structure remains visible in the pattern.

After annealing in argon for a short time (15 min) at 673 K (Fig. 4c), narrowing of all diffraction peaks occurred. This effect is evidently related to structural stress relaxation in the powder particles. Additionally, recovery of XRD lines characteristic of the αFe phase was observed. Simultaneously, the intensity of the Fe_3N peaks decreases, showing chemical instability of the iron nitride phase. For the sample annealed up to 1273 K the XRD pattern shows only peaks characteristic of αFe, so that the nitride undergoes thermal decomposition. The problem of thermal stability will be addressed below along with the results of DSC and TG analysis.

3.3. XRD analysis of ball-milled αFe–pyrazine mixtures

The results with pyrazine are dramatically different. Fig. 5 illustrates the changes in XRD patterns of αFe–pyrazine ball-milled powder after the two different milling times and annealing temperatures. Again, as discussed above for αFe–piperazine samples, the nitridation process exhibits major differences as compared with results obtained for αFe–NH_3 powders. As for piperazine, with pyrazine the nitriding process begins immediately on initiation of milling, with a parallel iron amorphization. However, for this mixture much higher reactivity can be observed. The XRD pattern for αFe–pyrazine powder milled for 144 h shows remarkable changes by comparison with

αFe–piperazine powder prepared with the same processing time. The nitridation process is much accelerated (cf. Figs 5a and 4a). Only the strongest peak (1 1 0) of the αFe structure is visible, but with decreased intensity; and additional peaks characteristic of the hexagonal Fe_3N structure occur. From the XRD pattern of Fig. 5a hexagonal unit cell values calculated were found to be $a = 0.2697$ nm and $c = 0.4360$ nm which agree well with tabulated data for Fe_3N. Next, for αFe–pyrazine powder milled for 288 h, the values of $a = 0.2687$ nm and $c = 0.4348$ nm obtained were found to be slightly smaller (dependent on the milling period). It is presumed that with the increased milling time the appearance of structural disorder influences these results. These effects disappear for annealed powder (milled for 288 h), and both structural parameters agree with tabulated values [15].

A short annealing time at 673 K was found to be beneficial in inducing the Fe_3N structure-ordering process. The observed XRD peak linewidth decreases, while the intensity remains at the same level (Fig. 5c). Heat treatment at an elevated temperature (1273 K) as before induces nitride decomposition, and as is shown in Fig. 5d, the XRD pattern shows the typical bcc αFe structure.

To sum up the XRD results on ball-milled αFe–pyrazine powders, it can be seen that for prolonged milling time the possibility exists of obtaining a pure Fe_3N phase. We remark that our starting powder stoichiometry was calculated for a $\gamma' Fe_4N$ phase as a final product. Thus, in the present experimental situation, where only the Fe_3N phase forms (instead of $\gamma' Fe_4N$), an additional 2.3 wt % of nitrogen is required for full iron nitridation to get 3:1 Fe:N ratio. Further preparations should be taken in accord with a 3:1 (Fe_3N) stoichiometry instead of the 4:1 ratio used. From recently reported results of αFe ball milling-nitridation in NH_3 [3, 4], and the present study, it is concluded that after reactive milling only one nitride phase can be formed directly, i.e. Fe_3N.

The tendency to form only the 3:1 phase during reactive milling with different nitridation agents seems to be a characteristic feature of this preparation method. It is surprising because other methods, such as annealing in a nitrogen-containing atmosphere, ion implantation, plasma evaporation or sputtering, are more able to yield a broad range of Fe–N compositions [7]. According to the Fe–N equilibrium phase diagram [16], which was recently summarized [7], we can expect the existence of four phases – αFe, $\gamma' Fe_4N$, Fe_3N and Fe_2N – with different proportions depending on the nitrogen content at temperatures below 860 K. Thus, room temperature reactive milling in a high N concentration environment should yield a stable multiphase system, i.e. $\gamma' Fe_4N$–Fe_3N. However, directly after preparation, in our experiments and others involving a NH_3-active atmosphere, for all XRD patterns, peaks associated with the γ' phase were not observed. It appears then, that the $\gamma' Fe_4N$ phase deficiency needs explanation. The limited work so far carried on bulk 4:1 and 3:1 phases has not resolved the controversy concerning the stability of both iron nitrides under mechanical activation. At present we can suggest only that a fcc Fe-atom arrangement in γ' Fe_4N, with N occupying one in four of the octahedral holes in a perfectly ordered manner (narrow phase homogenity 5.7–6.1 wt % N), cannot be synthesized by reactive milling. On the other hand, only the hcp Fe_3N structure, with a broader phase homogenity range, 8.25–11 wt % N, seems to be favourable.

3.4. Differential scanning calorimetry (DSC) and thermogravimetric analysis (TGA)

Thermal analysis was performed on as-prepared powders after milling for 288 h. For αFe–piperazine and αFe–pyrazine milled powders DSC scans were similar up to 673 K. The main feature is an endothermic peak in the low temperature range, up to ca. 390 K, with a sharp minimum at 373 K for the αFe–piperazine mixture. The peak for αFe–pyrazine at 355 K is broad. It is assumed that the highly hygroscopic nature of as-milled samples is responsible for the appearance of these peaks, because water molecules can be easily absorbed even during the short transfer and preparation time period to thermal analysis. DSC scans in the higher temperature range between 390 and 673 K show a flat characteristic of no interest for both samples.

More quantitative information can be deduced from TGA. For αFe–piperazine mixtures milled for both 144 and 288 h, TGA scans are shown in Fig. 6. For the 144 h ball-milled sample there are three characteristic temperature ranges where the TGA curve shows weight changes. In the first temperature range (I), up to 412 K, fast water desorption and piperazine decomposition takes place. The high value of observed weight loss (18.44 wt %) is larger than the amount of piperazine in the starting mixture (16.2 wt %) and this difference is due to absorbed water (estimated ca. 6 wt %). In the second temperature range (II), 412–908 K, a stable region up to ca. 720 K was observed and, subsequently, between 720 and 908 K further weight decrease (3.43 wt %) occurred. The last feature is characteristic for all prepared powders and can be assumed to be due to nitride decomposition. This assumption is certainly firmly based for all other samples where the XRD patterns show iron nitride diffraction lines as compared to the αFe–piperazine mixture milled for 144 h where only broad peaks from bcc iron are visible. Further experiments on the nitride phase formation are necessary to fully resolve this problem. For the moment it is supposed that crystalline nitride formation is taking place through a disordered phase – formed due to chemical bonding between nitrogen and iron atoms on the particle surfaces. In the next stages of milling, typical processes of mechanical alloying occur due to nitrogen diffusion. Thus, when the local concentration of N atoms reaches the critical value required for stable iron nitride compound formation the process of precipitation of a new crystalline phase occurs. Finally, in the third temperature region (Fig. 6a, III) a slow weight increase of 3.20 wt % was observed. Presumably, in this temperature range the remaining highly reactive iron powder

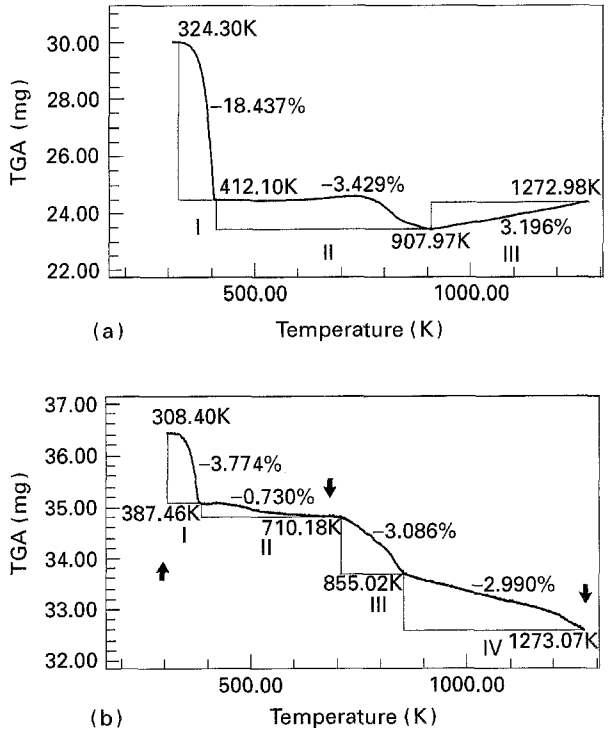

Figure 6 TGA curves of αFe–piperazine mixture milled for: (a) 144 h; (b) 288 h. The arrows indicate temperatures where XRD patterns were obtained (cf. Fig. 4).

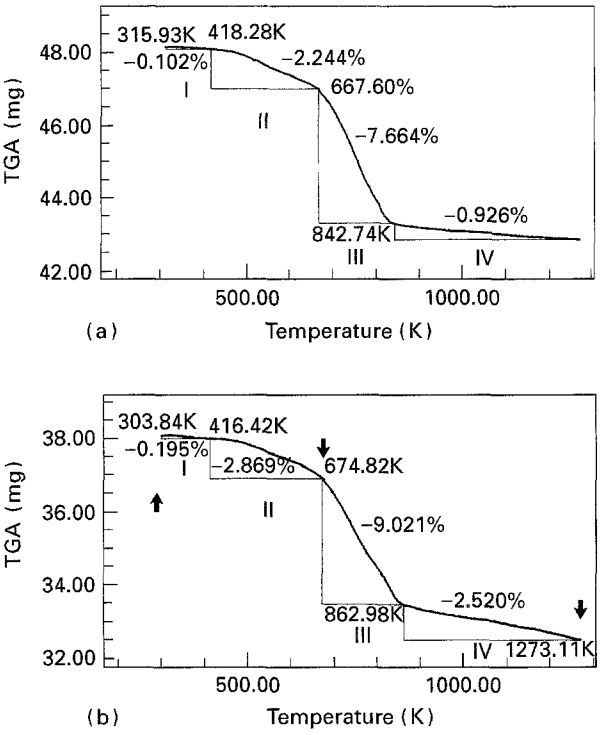

Figure 7 TGA curves of αFe–pyrazine mixture milled for: (a) 144 h; (b) 288 h. The arrows indicate temperatures where XRD patterns were obtained (cf. Fig. 5).

is influenced by oxygen as a contaminant from flowing argon gas used during the TGA experiment.

In Fig. 6b a TGA scan for 288 h milled powder is shown. The main features are broadly similar to results discussed above for a 144 h milled sample. However, as is clear from XRD analysis, the nitridation process was highly advanced in the longer milled sample. Accordingly, this TGA scan should confirm a pre-existing difference in chemical composition. Comparing TGA scans Fig. 6a and b we note the difference in temperature regions where the main features show up. There is a low temperature region (I) where desorption of H_2O^- molecules and/or piperazine decomposition ends at 387 K. Effective sample weight loss is smaller in Fig. 6b (3.77 wt %). In the second part (II) up to 710 K a further slow decomposition of the milled mixture takes place. In this temperature range release of hydrocarbon groups from the powder is the most probable source of this effect (0.73 wt %). The next region (III), temperature range 710–855 K, shows Fe_3N decomposition. In the last part of TGA scan Fig. 6b, (IV) a further decrease in weight (2.99 wt %) was observed. Taking into account the different chemical processes that occur, it is expected that oxidation occurs in this temperature range. However, rather than an increase in overall sample weight for iron, observed and described above for the 144 h milled powder, here we expect that carbon dissolved and/or existing on the particle surface reacts with oxygen to form CO or CO_2 gaseous molecules to provide the final weight decrease (2.99 wt %). As was recently found for other transition metal group powders milled with the same organic compounds [17], the effect of carbon contamination has great importance in preventing oxidation in the high temperature range. Additional study was undertaken to obtain more detailed information concerning its mechanism.

In Fig. 7 TGA scans for both αFe–pyrazine mixtures, milled for both 144 and 288 h, are presented. The shape of TGA curve for both powders is similar, and the only differences are observed in overall intensity and the temperature regions in which weight changes occur. As before, the whole scan can be divided into four temperature regions (cf. Figs 6 and 7). The most significant difference between powders prepared with piperazine and pyrazine is their behaviour in the first temperature region. For αFe–piperazine powders it has already been concluded that weight loss up to ca. 6 wt % at temperatures below 412 K is due to water adsorption before the experiment. [We remark additionally that piperazine easily forms a hexahydrate (+ $6H_2O$) molecule at room temperature, unlike pyrazine which does not form hydrates.] It is easy to understand that with the progressive milling time and tridation the amount of piperazine molecules available in the mixture decreases, along with adsorbed water. This as can be seen in Fig. 6. For the αFe–pyrazine mixture two observations are made: (1) the process of nitridation is apparent even after 144 h and the amount of remaining pyrazine molecules is reduced; and (2) that the pyrazine powder is less hygroscopic. The values of weight loss observed in Fig. 7 in the I temperature region are extremely low (up to 0.2 wt %). The second temperature region, 416–670 K, was found to be milling-time independent and both values of weight loss are similar (2.9–2.2 wt %). The most interesting changes were observed in temperature regions III and IV, where with the longer milling time the observed weight losses increased. As above, the process of Fe_3N decomposition can be linked with

weight loss in temperature region III and the value 9.0 wt % for 288 h milled powder is in good agreement with that expected for a pure Fe_3N phase with a nitrogen concentration value of 8.36 wt %. The measured value is slightly higher, but still in the stability range for a 3:1 phase (< 11.0 wt % N). For the last temperature region in TGA scans of αFe–pyrazine powders a decrease of weight depending on the milling time was observed. The values found were − 0.93 and − 2.52 wt % for 144 and 288 h milled powders, respectively. As we remarked before, oxidation of the remaining carbon from the amine compound is probably responsible for the detected weight loss. With the longer milling time the intensity of the effect increases in parallel with the amount of dissolved carbon. XRD patterns do not show peaks characteristic of any known stoichiometric Fe–C compound and formation of the crystalline form has to be discounted. Additionally, from the Fe–C phase diagram [16] it is known that solid solution in the wide carbon concentration range (0–5 wt %) exists normally in the temperature range up to ca. 1000 K. Thus, the problem of carbon localization (dissolved or between grains), as well as formation of a stable iron carbide Fe_3C side by side with Fe_3N [18], requires further study. It is currently under investigation and will be addressed in the future.

4. Summary

Mechanically-activated solid state synthesis reactions between elemental αFe powder and piperazine ($H_{10}C_4N_2$) and pyrazine ($H_4C_4N_2$) have been studied. Powder samples prepared after 144 and 288 h of ball milling in vacuum were examined by X-ray diffraction, scanning electron microscopy and thermal analysis methods. Formation of a Fe_3N crystalline phase was observed for as-prepared 288 h milled powders. The amount of nitride phase occurring depends on milling time and annealing temperature, and the overriding determinant is the chemical structure of the amine compound used. Pyrazine was found to be a superior nitriding agent which can be used for preparations involving ball-milling techniques. High content of nitrogen per molecule, relatively fast direct nitriding action (compared with NH_3 gas) because a higher surface density can be maintained during the milling process, and lack of hygroscopic properties are the main advantages of pyrazine in the applications studied. Even the twice higher bond dissociation energy for N-C chemical bonds in amine molecules as compared with the N-H type in ammonia has no obvious influence because the time required for Fe_3N formation is relatively shorter for the αFe–pyrazine mixture. Further experiments are being undertaken to produce a pure Fe_3N phase by improvements in the technology. Other amine compounds are being used in preparations to obtain more information about the chemical synthesis mechanism.

Acknowledgements

The authors appreciate the useful experimental assistance of Z. Li with the thermal analysis. This research has been carried out on behalf of the Harry Triguboff AM Research Syndicate.

References

1. L. E. TOTH "Transition metal carbides and nitrides", Refractory Materials Series, Vol. 7 (Academic Press, New York, 1972).
2. A. CALKA and J. S. WILLIAMS, *Mater. Sci. Forum* **88–90** (1992) 787.
3. T. KOYANO, C. H. LEE, T. FUKUNAGA and U. MIZUTANI, *ibid.* **88–90** (1992) 809.
4. K. MAJIMA, M. ITOH, S. YAGYU, S. KATSUYAMA and H. NAGAI in Proceedings of 1993 Powder Metallurgy World Congress, Japanes Society of Powder Metallurgy (1993) p. 706.
5. S. MATAR, *Zeitschrift Phys.* B **87** (1992) 91.
6. J. M. D. COEY, K. O'DONNELL, QI QINIAN, E. TOUCHAIS and K. H. JACK, *J. Phys. Condens. Matter* **6** (1994) L23.
7. K. H. JACK, *J. Appl. Phys.* **76** (1994) 6620.
8. S. MATAR, B. SIBERCHICOT, M. PÉNICAUD and G. DEMAZEAU, *J. Physique* **2** (1992) 1819.
9. S. K. CHEN, S. JIN, T. H. TIEFEL, Y. F. HSIEH, E. M. GREGORY and D. W. JONHNSON, *J. Appl. Phys.* **70** (1991) 6247.
10. D. ANDRIAMANDROSO, S. MATAR, G. DEMAZEAU and L. FOURNES, *IEEE Trans. Magn.* **29** (1993) 2.
11. X. BAO, R. M. METZGER and W. D. DOYLE, *J. Appl. Phys.* **73** (1993) 6734.
12. P. ETTMAYER and W. LENGAUER, NITRIDES, in "Ullmann's encyclopedia of industrial chemistry" edited by B. Elvers (VCH Verlagsgesellschaft, Weinheim, 1991) **A17**, p. 353.
13. Distributed by Anutech Pty. Australian National University.
14. W. A. KACZMAREK and B. W. NINHAM, *IEEE Trans. Magn.* **30** (1994) 732.
15. JCPDS–ICDD Database (1992) File no. 1–1236.
16. M. HANSEN and K. ANDERKO, "Constitution of binary alloys" (McGraw-Hill, New York, 1958) p. 670.
17. W. A. KACZMAREK and I. ONYSZKIEWICZ, *Mater. Sci. Forum* **179–181** (1995) 195.

Received 14 June 1994
and Accepted 5 April 1995